ACS OMEGA

http://pubs.acs.org/journal/acsodf

Article

Fabrication of PEBA/HZIF-8 Pervaporation Membranes for High Efficiency Phenol Recovery

Yan Xue Xue, Fei Fei Dai, Qian Yang,* Jian Hua Chen, Qiao Jing Lin, Li Jun Fang, and Wei Wei Lin

Cite This: *ACS Omega* 2022, 7, 23467−23478

Read Online

ACCESS | Metrics & More | Article Recommendations

ABSTRACT: Phenol and its chemical derivatives serve as essential chemical materials are indispensable for the synthesis of many kinds of polymers. However, they are highly toxic, carcinogenic, difficult to be degraded biologically, and often found in aqueous effluents. Recovery of hazardous phenol from wastewater remains a daunting challenge. Herein, we prepared a hybrid membrane containing polyether block amide (PEBA) matrix and HZIF-8 fillers. To improve the compatibility between ZIF-8 and PEBA, ZIF-8 was modified by using polystyrene (PS) as a template to prepare porous HZIF-8. ZIF-8, composed of zinc nodes linked by the imidazole ring skeleton, is a kind of inorganic material with high hydrothermal stability, ordered pores, and hydrophobic microporous surfaces, which has a wide range of applications in membrane separation. The separation performance of the PEBA/HZIF-8 based membranes for phenol/water is improved due to the presence of PS on the surface of HZIF-8 and the imidazole ring skeleton in ZIF-8, which enhance the $\pi-\pi$ interaction between HZIF-8 and phenol molecules. The effects of HZIF-8 content, feed phenol concentration, and feed temperature on the pervaporation performance of PEBA/HZIF-8 membranes were further investigated. The results showed that the pervaporation performance of the PEBA/HZIF-8-10 membrane was promising with a separation factor of 80.89 and permeate flux of 247.70 g/m^2·h under the feed phenol concentration of 0.2 wt % at 80 °C. In addition, the PEBA/HZIF-8-10 membrane presented excellent stability, which has great prospect for practical application in phenol recovery from waste water.

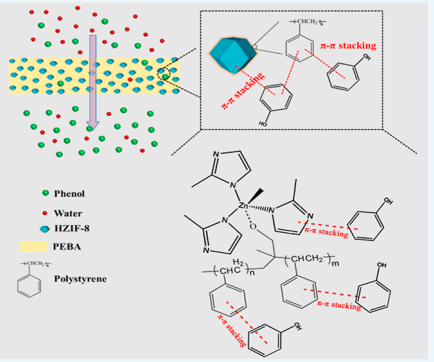

1. INTRODUCTION

Phenolic compounds are of great importance in many industrial processes, for example, phenol is an indispensable organic chemical raw material for the synthesis of diphenyl propane,[1] 4-amino-2-fluorophenol,[2] anisole,[3] picric acid,[4] and bakelite (phenolic resin).[5] Due to the lack of efficient recovery technology for phenol and its derivatives, they are usually found in the wastewater produced by many chemical plants, which is currently one of the most concerning environmental issues.[6] Phenol is a highly toxic substance and not easily biodegraded at high concentrations (>200 mg/L).[7] What is more, it will do harm to human health at low concentration levels.[8] The World Health Organization (WHO) recommends that the allowable phenol concentration in drinking water is <0.001 mg/L.[9] The Environmental Protection Agency has restricted the concentration of phenol in industrial wastewater to less than 1 mg/L before it can be discharged into surface water.

Considering the industrial application and the harm to the environment and human body, it is of great significance for the separation and recovery of phenol from dilute solution.[10] It is more difficult to recover phenol from the aqueous solution because the radius of a phenol molecule (0.6 nm)[11] is larger than that of a water molecule (0.27 nm).[12] At present, there are many methods to recover phenol from aqueous solution, such as adsorption,[13,14] electrodialysis,[15] photocatalytic,[16] biodegradation,[17,18] ultrasound-assisted electrochemical,[19] ozone oxidation,[20] and membrane separation technology.[21−23] However, these methods suffer from the problems of high cost, high energy consumption, easy to cause secondary pollution, and/or poor selectivity. Hence, it is an urgent need to find efficient technologies to recover phenolic compounds from wastewater.

Pervaporation has attracted wide attention as an alternative technology to remove low-concentration volatile organic compounds from wastewater, and it is considered to have broad industrial application prospects. First of all, the cost of pervaporation technology is much lower than that of distillation, and it is thus expected to replace the distillation and become the mainstream separation technology for liquid mixtures such as azeotropic mixtures, isomers, heat-sensitive compounds, and so forth.[24]

Received: March 26, 2022
Accepted: June 14, 2022
Published: June 27, 2022

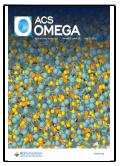

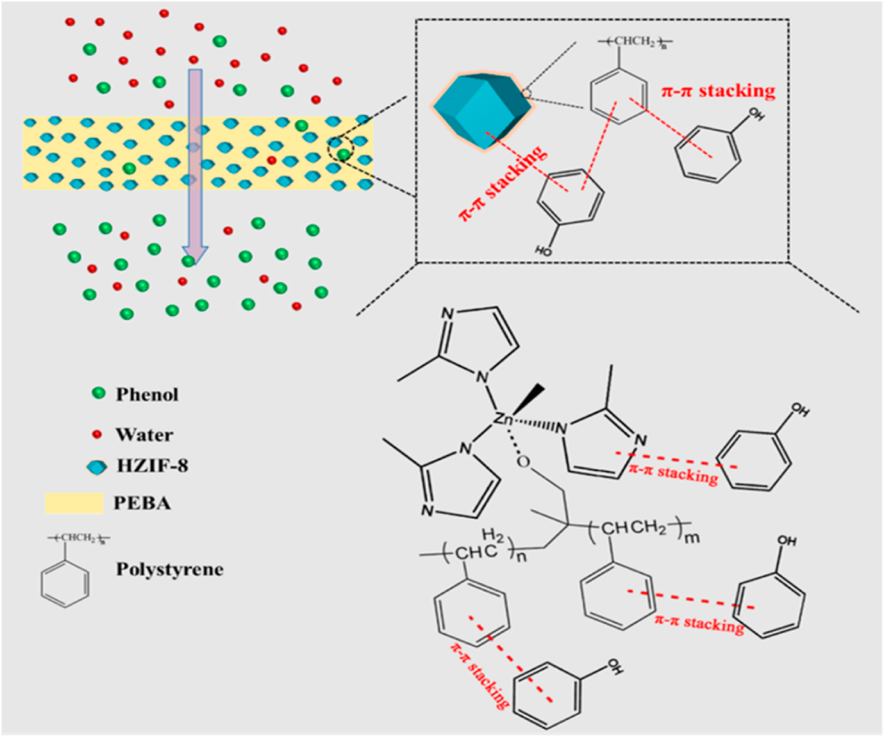

Figure 1. Schematic diagram of separation of phenol/water by PEBA/HZIF-8 membranes.

Polyether block amide (PEBA) is a kind of polymer material composed of regular hard polyamide chain segments and soft polyether chain segments, which has a high affinity with organic compounds.[25] Hao et al. used PEBA-2533 as a monomer material for the membrane separation of phenol and water. PEBA had excellent osmotic selectivity for phenol because it can interact with aromatic compounds through π-bond and preferentially adsorb aromatic compounds.[10] Zhang et al. prepared β-CD-f-PEBA membranes by adding β-CD into PEBA and applied in the pervaporation separation of phenol/water. When the β-CD content achieved 0.5 wt %, the total osmotic flux and separation factor were 319.3 g/m^2·h and 43.3, respectively.[26] Khan et al. prepared a mixed matrix membrane by incorporating MAF-6 as a filler into the PEBA polymer for pervaporation of separation of phenol/water. The optimum separation coefficient of MAF-6-7@MMM was 25.9, and the phenol flux was 89.2 g/m^2 at 80 °C and 1000 ppm of phenol solution.[27] Further research on the performance of membrane materials is the key to the development of membrane separation technology. At present, most of the research is devoted to the modification of membrane materials and the development of pervaporation membranes with higher separation performance. The focus of the pervaporation process is on the selection of membrane materials, and so, a PEBA-based membrane was chosen in this paper. However, the flux, selectivity, or stability of the PEBA-based membrane still should be improved. Recently, to further improve the pervaporation performance of PEBA-based membranes, inorganic materials, such as metal−organic frameworks[28,29] and zeolite molecular sieves,[30,31] have been incorporated into the PEBA matrix to fabricate hybrid membranes, which possess the advantages of both pure polymer and pure inorganic. Zeolite imidazole ester framework materials (ZIFs) have attracted great attention in many fields such as gas storage and separation due to their high specific surface area, regulable pore structure, and pore functionality.[31−33] The imidazole ring framework in ZIF-8 can form $\pi-\pi$ interaction with phenol. However, the direct combination of ZIF-8 and PEBA has the problem of incompatibility between polymer and pure inorganic.[34−36] To solve this problem, the high hydrophobic porous HZIF-8 is synthesized by using polystyrene (PS) as a template, and then, PEBA/HZIF-8 membranes were prepared for the separation of phenol in water by pervaporation (Figure 1). PS was used to adjust the aperture and crystal surface hydrophobicity of HZIF-8 to provide a larger channel and hydrophobic environment simultaneously. The introduction of PS could improve the compatibility between HZIF-8 and PEBA polymer and the $\pi-\pi$ interaction between PEBA/HZIF-8 membranes and phenol molecules, and therefore, the mass transfer ability of phenol molecules across the membrane was significantly enhanced.

2. EXPERIMENTAL SECTION

2.1. Materials. Polyether block polyamide (PEBA, grade of 2533) was purchased from French Arkema Co., Ltd. *N*,*N*-dimethylacetamide (DMAc, AR) and 2-methylimidazole (Hmim, 98%) were purchased from Shanghai McLean Biochemical Technology Co., Ltd. Phenol (C_6H_5OH, AR), $Zn(NO_3)_2{\cdot}6H_2O$ (AR), methanol (CH_3OH, AR), styrene (AR), methacrylic acid (CP), $K_2S_2O_8$ (AR), *N*,*N*-dimethylformamide (DMF, AR), and ethanol (C_2H_5OH, AR) were obtained from Xilong Chemical Co., Ltd. All reagents were used without further purification.

2.2. Preparation of PS and HZIF-8. The preparation of PS and HZIF-8 was based on the previous work by Peng et al. with minor modifications.[44] PS was synthesized by the following steps: A solution of styrene (54 mL), methacrylic acid (MAA, 6 mL), and deionized water (450 mL) was mixed under stirring at 80 °C. After a homogeneous solution was formed, an aqueous solution (30 mL) containing $K_2S_2O_8$ (0.6

https://doi.org/10.1021/acsomega.2c01847
ACS Omega 2022, 7, 23467−23478

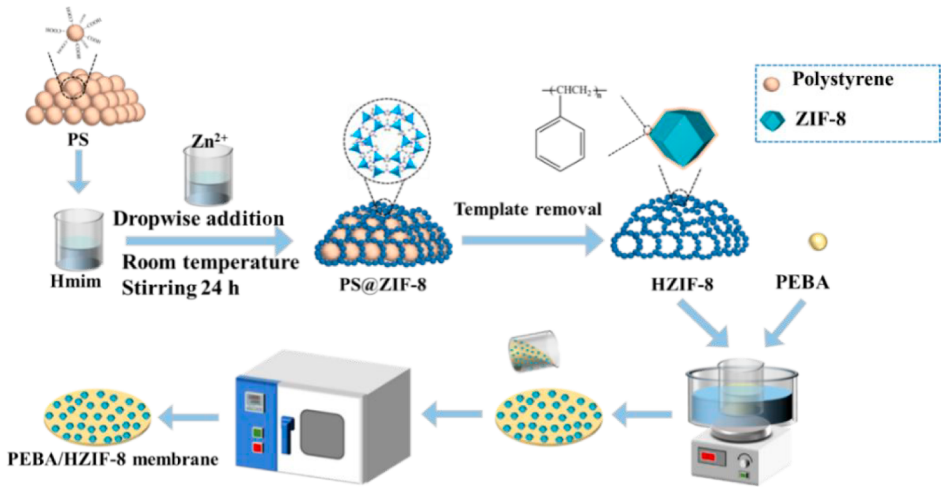

Figure 2. Preparation of HZIF-8 and PEBA/HZIF-8 membranes.

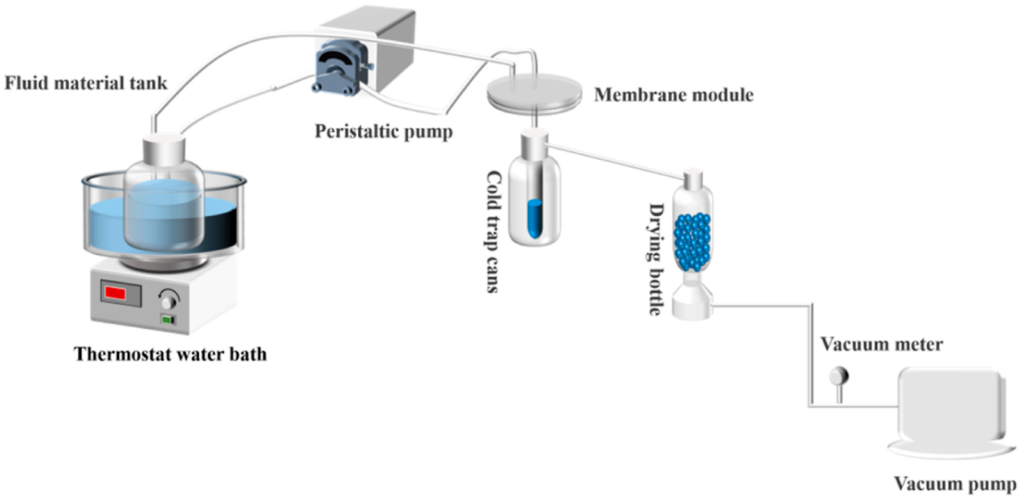

Figure 3. Schematic diagram of the pervaporation experiment device.

g) was added and then stirred for 24 h. After centrifugation at 10,000 rpm, the PS microspheres were separated from the solution and washed with 50 mL of ethanol and 50 mL of deionized water for six times. Finally, the product was dried at 60 °C to obtain PS microspheres.

HZIF-8 was prepared by the following procedure: PS (0.2 g) was added to a solution of 2-methylimidazole (1.311 g) in methanol (58 mL). $Zn(NO_3)_2{\cdot}6H_2O$ (0.298 g) in methanol (2 mL) was added dropwise to the above solution, and then, it was stirred at room temperature for 24 h. The crude product was collected by centrifugation at 10,000 rpm and washed with ethanol. Finally, *N*,*N*-dimethylformamide (20 mL) was added to the crude product and stirred at 80 °C for 24 h to remove the PS template. The product was separated by suction filtration, washed with 30 mL of ethanol for seven times, and finally dried under vacuum at 150 °C for 12 h to obtain HZIF-8. During the reaction, Zn^{2+} first coordinated with the carboxyl group on the PS surface and then coordinated with 2-methylimidazole.

2.3. Preparation of PEBA/HZIF-8 Pervaporation Membranes. The preparation processes of PEBA/HZIF-8 membranes are shown in Figure 2. A certain quantity of HZIF-8 (the content of HZIF-8 was 0, 2.5, 5, 10, and 12 wt % of the PEBA mass, respectively) was added into DMAc (19.8 g). After completely dispersed, PEBA (2.2 g, 10 wt %) was added to the above solution and then stirred at 80 °C for 4 h. After degassing to remove bubbles, the solution was cast on the glass plate to prepare membranes, left at room temperature overnight, and then dried in the oven at 70 °C for 24 h, followed by further vacuum drying at 50 °C for 12 h. The prepared membranes were named as PEBA/HZIF-8-0, PEBA/HZIF-8-2.5, PEBA/HZIF-8-5, PEBA/HZIF-8-10, and PEBA/HZIF-8-12.

2.4. Characterization of HZIF-8 and PEBA/HZIF-8 Membranes. The surface and section of PEBA/HZIF-8 membranes and the morphology of HZIF-8 were characterized by a scanning electron microscope (SEM) (JSM-6010LA model, Japan). Before the SEM test, the samples were coated with gold by a sputter coater to improve their conductivity for obtaining good quality of micrograph. The structures of ZIF-8, HZIF-8, and PEBA/HZIF-8 membranes were analyzed by X-ray diffraction (XRD, Ultimaiv model, Neo-Japanese, Bruker D8 Advance, Cu K-a radiation, the current/voltage is 40 mA/40 kV). Fourier transform infrared spectroscopy (FT-IR, Nicolet IS10, Thermo Fisher Company, USA) was used to analyze ZIF-8, HZIF-8, PS, PS@ZIF-8, and PEBA/HZIF-8 membranes with the scanning spectrum range of 380−4000 cm^{-1}. An atomic force microscope (AFM, CSPM5500,

https://doi.org/10.1021/acsomega.2c01847
ACS Omega 2022, 7, 23467−23478

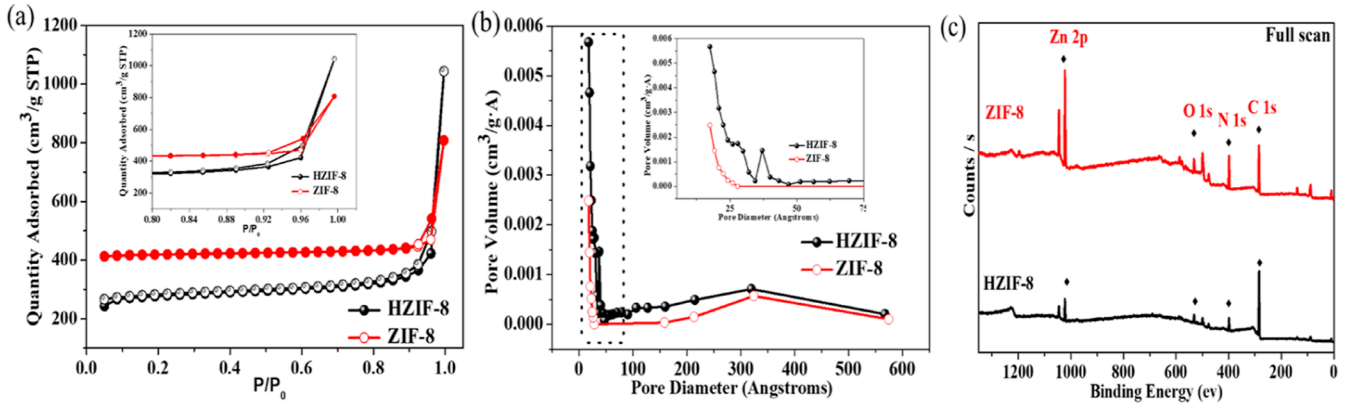

Figure 4. BET and XPS analysis of ZIF-8 and HZIF-8: (a) N_2 adsorption−desorption isotherm at 77 K (the illustration showed the enlarged area at $P/P_0 > 0.8$), (b) aperture distribution diagram, and (c) XPS total spectrum analysis diagram.

Guangzhou Benyuan Nanoinstrument Co., Ltd.) was used to analyze the surface structure and roughness of PEBA/HZIF-8 membranes. The elemental composition and chemical state of HZIF-8 and ZIF-8 were analyzed by X-ray photoelectron spectroscopy (XPS, Thermo Escalab 250XI, Thermo Eisenhower Science). The specific surface area and pore size distribution of ZIF-8 and HZIF-8 were analyzed by BET (Gemini 2390 ISN#626, McMuritic Instruments Co., Ltd.) with N_2. A dynamic/static contact angle meter (SL200B, Kono Industries, USA) was used to test the hydrophobicity of ZIF-8, HZIF-8, and PEBA/HZIF-8 membranes by the pendant drop method. Deionized water was used as the test liquid, and the hydrophobicities of ZIF-8, HZIF-8, and PEBA/HZIF-8 membranes were measured according to the hanging drop method, and each sample was tested for an average of three times to ensure the accuracy of the contact angle.

2.5. PEBA/HZIF-8 Membrane Pervaporation Experiments. The experimental apparatus for recovery of phenol by pervaporation was performed in a laboratory-scale setup, as shown in Figure 3. The membrane assembly consists of a circular component with a radius of 8 cm. The feed was transported to the upstream of the membranes through a peristaltic pump and circulated on the surface of the membranes. The downstream of the membranes was evacuated by a vacuum pump, and the pressure was kept below 100 Pa. The effective area of the membranes was 63.6 cm^2. The flow rate of the feed solution (0.2−0.8 wt % phenol concentration) was 160 cm^3/min, and the temperatures of the feed ranged from 30 to 80 °C. After stable operation of the device, the permeate was collected by using the −50 ethylene glycol solution (80 wt %) as the cold trap liquid. Permeate feed was collected every 0.5 h. The quantitative analysis of phenol concentration in the permeate was determined by a UV−Vis spectrophotometer (UV-1600PC, Shanghai Mapode Instrument Co., Ltd). The absorbance of phenol was recorded at their λ_{max} = 267 nm.

Pervaporation performance of PEBA/HZIF-8 membranes for phenol separation was mainly evaluated by total permeation flux (J) (g/m^2·h) and separation factor (β). To evaluate the overall pervaporation performance of PEBA/HZIF-8 membranes, the percolation separation coefficient (PSI) was also used, as shown in eq 3, which took into account both the separation factor and the total flux.

$$J = \frac{m}{A \cdot t} \tag{1}$$

$$\beta = \frac{Y_A \cdot X_B}{Y_B \cdot X_A} \tag{2}$$

$$\mathrm{PSI} = J \cdot (\beta - 1) \tag{3}$$

where m (g) was the weight of the permeate collected in time t (h), and A (m^2) was the effective membrane area. X_A (wt %) and X_B (wt %) were the contents of phenol and water in the feed solution, respectively. Y_A (wt %) and Y_B (wt %) were the contents of phenol and water in the permeate solution, respectively.

2.6. Swelling Test of PEBA/HZIF-8 Membranes. PEBA/HZIF-8 membranes were vacuum dried at 50 °C for 12 h and then weighed. The weight of the dried membrane was recorded as M_0 (g). The dried membranes were immersed in 0.8 wt % phenol aqueous solution at 70 °C to reach adsorption equilibrium. After that, the membranes were removed and the solution on the surface of the membranes was quickly wiped with absorbent paper and weighed and denoted as M (g). The swelling degree (SD) was calculated by eq 4.

$$\mathrm{SD} = \frac{M - M_0}{M_0} \tag{4}$$

The adsorption selectivity (α_s) of PEBA/HZIF-8 membranes was evaluated by eq 5.

$$\alpha = \frac{M_P \cdot F_W}{M_W \cdot F_P} \tag{5}$$

where M_W (wt %) and M_P (wt %) are the contents of water and phenol adsorbed in the membrane, respectively; F_W (wt %) and F_P (wt %) are the contents of water and phenol in the feed solution, respectively.

The diffusion selectivity (α_d) of membrane was evaluated by eq 6.[37]

$$\alpha_d = \frac{\beta}{\alpha_s} \tag{6}$$

3. RESULTS AND DISCUSSION

3.1. Characterization. *3.1.1. BET and XPS Analysis of ZIF-8 and HZIF-8.* The specific surface area and pore size distribution of HZIF-8 and ZIF-8 were characterized by BET using N_2 adsorption isotherm at 77 K. As shown in Figure 4a, the samples all exhibit I-type isotherms lower than P/P_0 = 0.1, indicating that both ZIF-8 and HZIF-8 had microporous

https://doi.org/10.1021/acsomega.2c01847
ACS Omega 2022, 7, 23467−23478

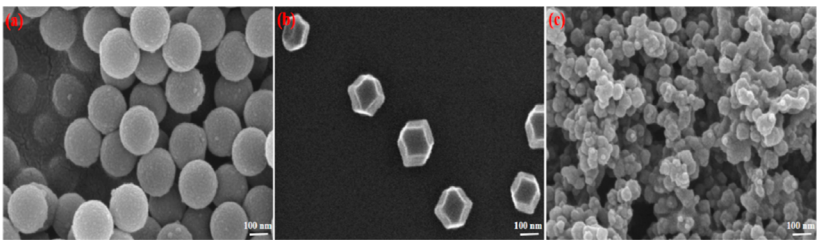

Figure 5. SEM images of (a) PS, (b) ZIF-8, and (c) HZIF-8.

structures. At P/P_0 > 0.85, the absorption of N_2 increased sharply, which may be caused by the existence of gaps between the particles. As shown in Figure 4b, ZIF-8 mainly contained micropores, while HZIF-8 possessed both micropores (<2 nm) and mesopores (the average pore size was about 7.48 nm). The formation of mesopores was induced by the aggregation of HZIF-8 nanocrystals. The specific surface areas of ZIF-8 and HZIF-8 were 1265.40 and 863.65 m^2/g, respectively. The low specific surface area of HZIF-8 was attributed to the existence of mesopores.

The element information and chemical composition of ZIF-8 and HZIF-8 were analyzed by XPS, as shown in Figure 4c. Both ZIF-8 and HZIF-8 contained Zn, O, N, and C elements. Compared with the total XPS spectrum of ZIF-8, the peak intensity of Zn $2p_{3/2}$ and Zn $2p_{1/2}$ of HZIF-8 was weaker, while the peak intensity of C 1s was higher, indicating that the surface of HZIF-8 was successfully modified by PS.

3.1.2. Scanning Electron Microscopy Analysis. The morphology of PS, HZIF-8, and ZIF-8 was analyzed by SEM characterization. As shown in Figure 5a–c, PS showed a regular spherical structure, while ZIF-8 presented a regular rhomboid dodecahedron shape, which was consistent with the reported literature.[35] The ZIF-8 growth on the surface of PS 280 spheres restricted the growth of particles, resulting in 281 the lower size of HZIF-8 in comparison with those of PS and 282 ZIF-8. As shown in Figure 5c, HZIF-8 gather to form a three-dimensional network structure, indicating the successful fabrication of HZIF-8.

The surface and cross-sectional morphology of PEBA/HZIF-8 based membranes were observed by SEM. The thickness of the prepared membranes were in the range of 80–90 μm. As shown in Figure 6a–b, the PEBA/HZIF-8-0 membrane presented a smooth and defect-free surface. With the increase of HZIF-8 content, more HZIF-8 were distributed on the membrane surface, leading to the increase of roughness (Figure 6c–h). It should be noted that agglomeration of HZIF-8 occurred when the HZIF-8 content exceeded 10 wt %, and non-selective voids formed between the HZIF-8 and PEBA matrix, as shown in Figure 6i–j.

3.1.3. XRD Analysis and FT-IR. The crystal structures of ZIF-8 and HZIF-8 were characterized by XRD. As shown in Figure 7a, the diffraction peaks at 7.32, 10.55, 12.77, 14.69, and 18.22° represented (011), (002), (112), (022), and (222) crystal faces of ZIF-8, respectively. The crystal structure of the prepared ZIF-8 was consistent with that reported in the literature.[36] The diffraction peaks of HZIF-8 crystal planes were consistent with that of ZIF-8, indicating that modified ZIF-8 by PS still had the same crystal structure as ZIF-8. In order to investigate the stability of HZIF-8 particles in phenol solution, HZIF-8 particles were immersed in the solution with a phenol concentration of 0.8 wt % at 70 °C for 3 days. It could be seen from Figure 7a that HZIF-8 showed good

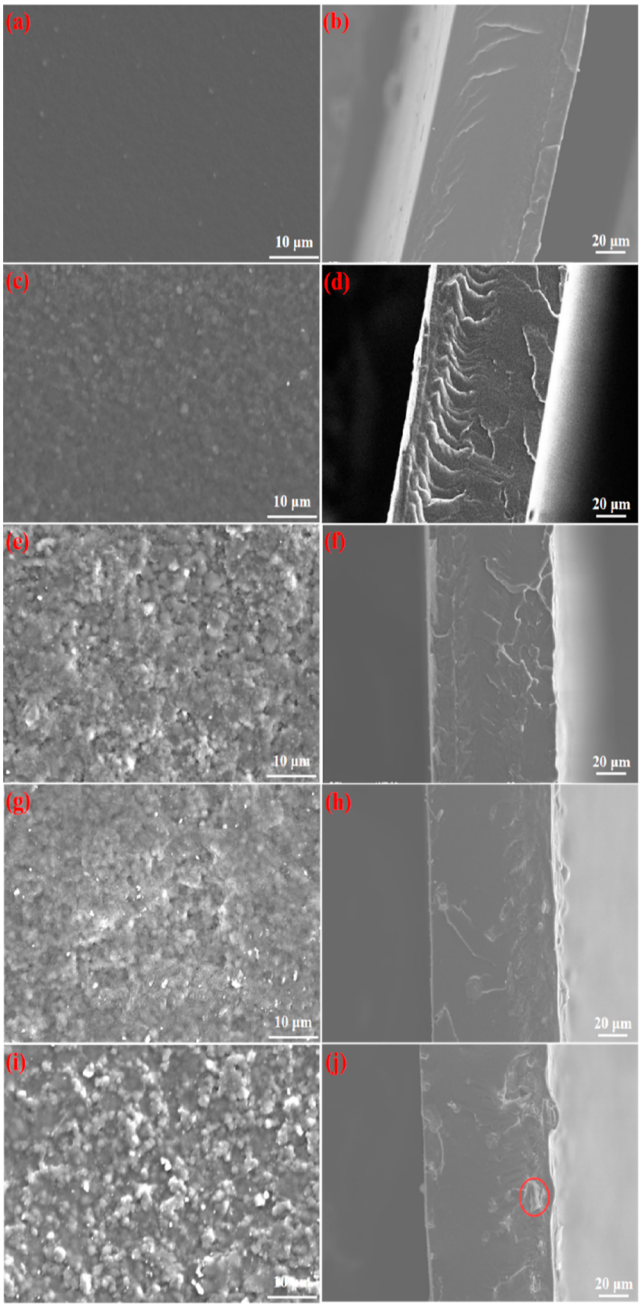

Figure 6. SEM images of surface and cross section of PEBA/HZIF-8 membranes: (a,b) PEBA/HZIF-8-0, (c,d) PEBA/HZIF-8-2.5, (e,f) PEBA/HZIF-8-5, (g,h) PEBA/HZIF-8-10, and (i,j) PEBA/HZIF-8-12.

stability. Figure 7b showed that the PEBA/HZIF-8-0 membrane had a wide peak at 2θ = 20°, which proved that

https://doi.org/10.1021/acsomega.2c01847
ACS Omega 2022, 7, 23467–23478

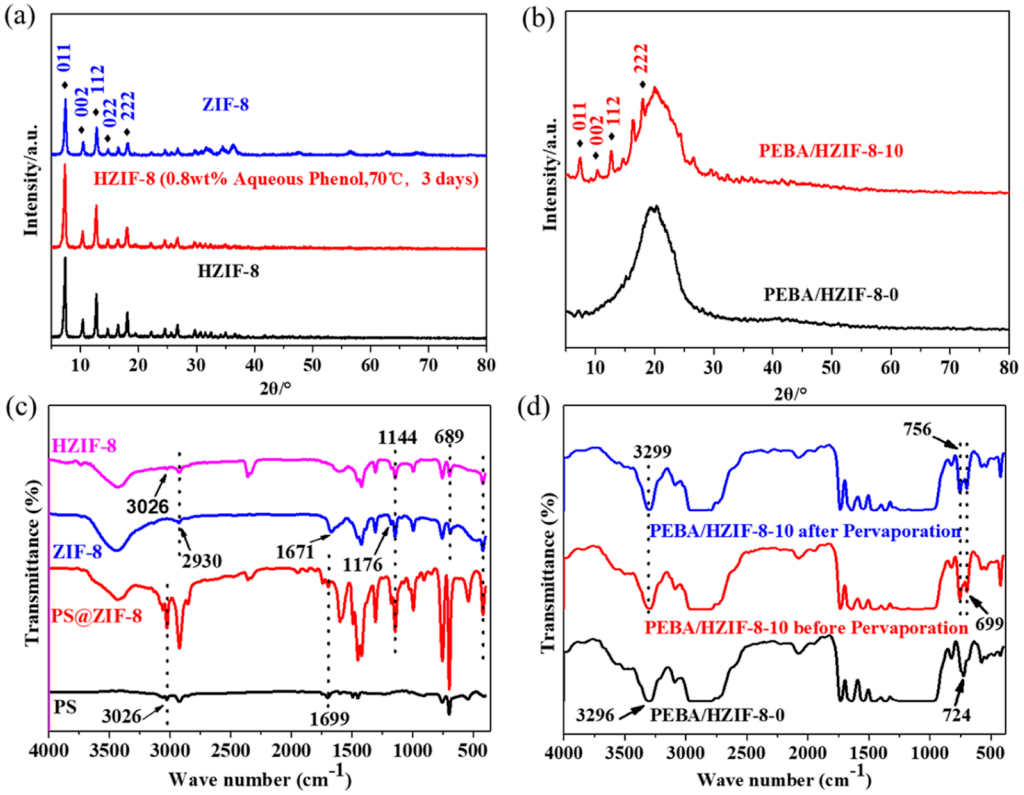

Figure 7. XRD patterns of (a) HZIF-8 and ZIF-8 and (b) PEBA/HZIF-8-0 and PEBA/HZIF-8-10; FT-IR spectra of (c) PS, PS@ZIF-8 (PS template had not been removed), ZIF-8, and HZIF-8, (d) PEBA/HZIF-8-0 and PEBA/HZIF-8-10 before and after pervaporation.

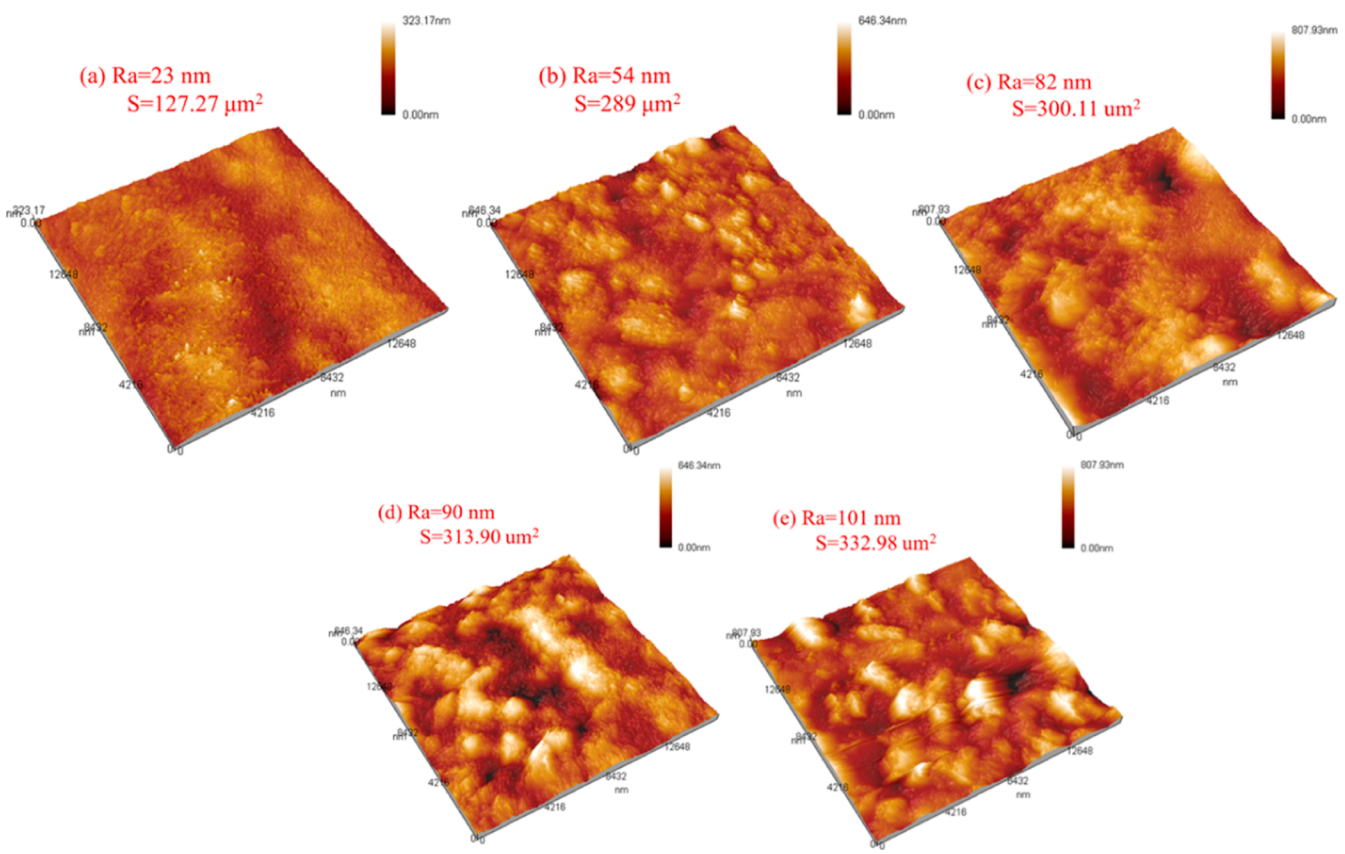

Figure 8. AFM diagram of PEBA/HZIF-8 membranes: (a) PEBA/HZIF-8-0, (b) PEBA/HZIF-8-2.5, (c) PEBA/HZIF-8-5, (d) PEBA/HZIF-8-10, and (e) PEBA/HZIF-8-12.

https://doi.org/10.1021/acsomega.2c01847
ACS Omega 2022, 7, 23467−23478

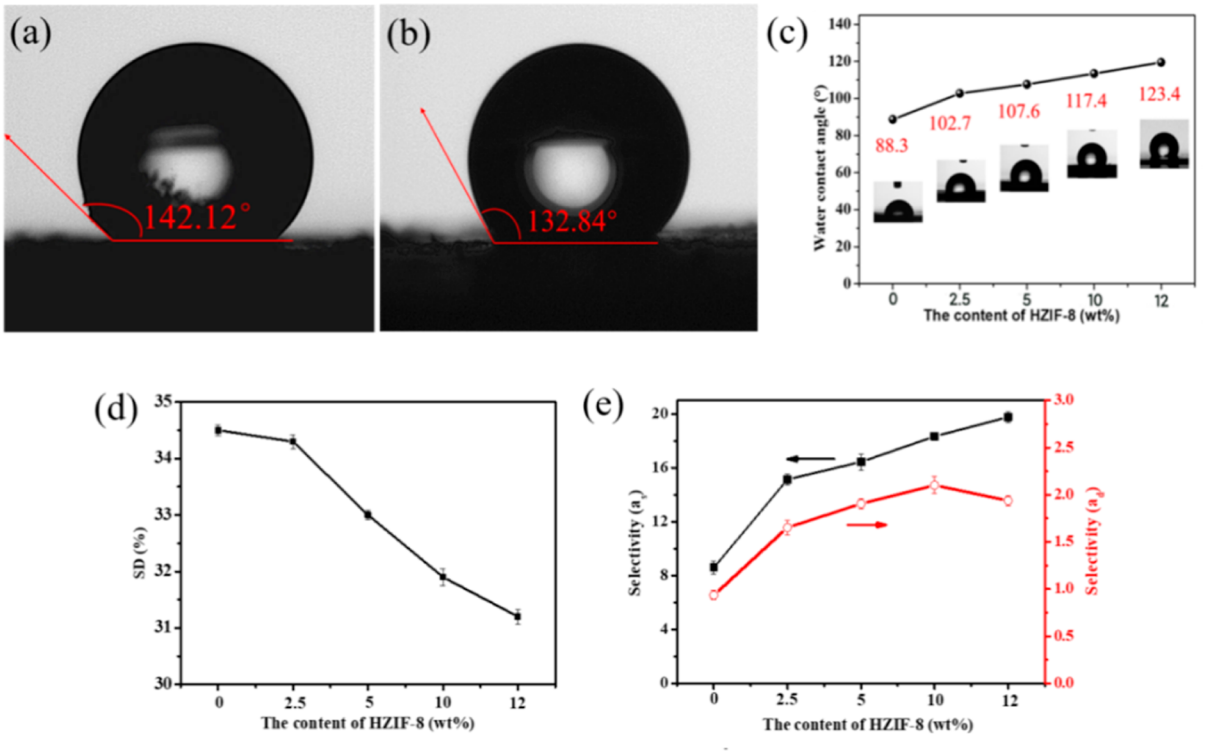

Figure 9. Water contact angle analysis: (a) HZIF-8 and (b) ZIF-8, and (c) effect of HZIF-8 content on the contact angle of PEBA/HZIF-8 based membrane surface; effect of HZIF-8 content on (d) SD, and (e) the adsorption selectivity(α_s) and diffusion selectivity (α_d) of PEBA/HZIF-8 membranes.

pure PEBA was amorphous. By comparing the spectra of PEBA/HZIF-8-0 and PEBA/HZIF-8-10 membranes, PEBA/HZIF-8-10 membranes retained the characteristic peaks of HZIF-8, indicating that the binding of HZIF-8 and PEBA could not change the skeleton structure of HZIF-8.

FT-IR was used to analyze the functional groups on the surface of the material and PEBA/HZIF-8-10 membranes. As shown in Figure 7c, the characteristic peaks of C−H (−CH_2−), C═N, and C−N bonds that belong to the imidazole ring of ZIF-8 located at 2930, 1671, 1176, and 1144 cm^{-1}.[38,39] The diffraction peak at 689 cm^{-1} was attributed to the stretching vibration of the Zn−N bond in ZIF-8,[19] and the diffraction peak at 1699 cm^{-1} was attributed to the stretching vibration of the C═O bond on −COOH. The spectrum of HZIF-8 retained the characteristic peaks of ZIF-8. In addition, a peak at 3026 cm^{-1} appeared, which was attributed to the stretching vibration of the C−H bond on the unsaturated carbon (the benzene ring). It demonstrated that the surface of HZIF-8 had been successfully modified with PS. In the infrared spectrum of the PEBA/HZIF-8-10 membrane, as shown in Figure 7d, the characteristic peaks of the Zn−O bond (756 cm^{-1}) and Zn−N bond (690 cm^{-1}) of HZIF-841,[40,41] could be observed, indicating that HZIF-8 retained its skeleton structure inside PEBA/HZIF-8 membranes. On comparing the infrared spectra of PEBA/HZIF-8-10 membrane before and after pervaporation, it could be observed that the characteristic peaks were basically unchanged. It could be concluded that the membrane had good stability.

3.1.4. Atomic Force Microscopy (AFM). The surface roughness of PEBA/HZIF-8 based membranes was analyzed by AFM. As shown in Figure 8, the surface of PEBA/HZIF-8-0 membrane was relatively smooth, showing a roughness (R_a) of 18 nm. With the increase of HZIF-8 content, the surface roughness of PEBA/HZIF-8 based membranes increased from 18 to 101 nm, and the corresponding surface area also increased. It is consistent with the SEM images. The contact areas between PEBA/HZIF-8 membranes and phenol were increased by the modification of HZIF-8, thus promoting the selective adsorption of phenol by PEBA/HZIF-8 based membranes.

3.1.5. Water Contact Angle Analysis and SD of PEBA/HZIF-8 Membranes. Water contact angle is used to evaluate the hydrophobicity of prepared membranes since it is a significant parameter that can affect the separation performance of membranes. PEBA/HZIF-8 based membranes with higher hydrophobicity possessed higher adsorption ability for phenol molecules on the membrane surface. As shown in Figure 9, HZIF-8 possessed high hydrophobicity (142.1°, Figure 9a), which was larger than that of ZIF-8 (132.8°, Figure 9b). With the increase of the content of HZIF-8 in hybrid PEBA/HZIF-8 membranes from 0 to 12 wt %, the water contact angles increased from 88.3 to 123.4° (Figure 9c).

The SD of PEBA/HZIF-8 based membranes was measured under 0.8 wt % phenol solution at 70 °C. As shown in Figure 9d, the SD of PEBA/HZIF-8 based membranes decreased gradually with the increase of HZIF-8 content. Because of the presence of high hydrophobic HZIF-8, the hydrophobicity of PEBA/HZIF-8 based membranes was improved and thus hindered the passage of water molecules through the membrane. In addition, with the increase of HZIF-8 content, the free volume between polymer chains of PEBA/HZIF-8 hybrid membranes decreased due to the insertion of HZIF-8.

The adsorption selectivity (α_s) and diffusion selectivity (α_d) of PEBA/HZIF-8 based membranes varied with HZIF-8 content, as shown in Figure 9e. The α_s of PEBA/HZIF-8 based membranes was significantly affected by the addition of

https://doi.org/10.1021/acsomega.2c01847
ACS Omega 2022, 7, 23467−23478

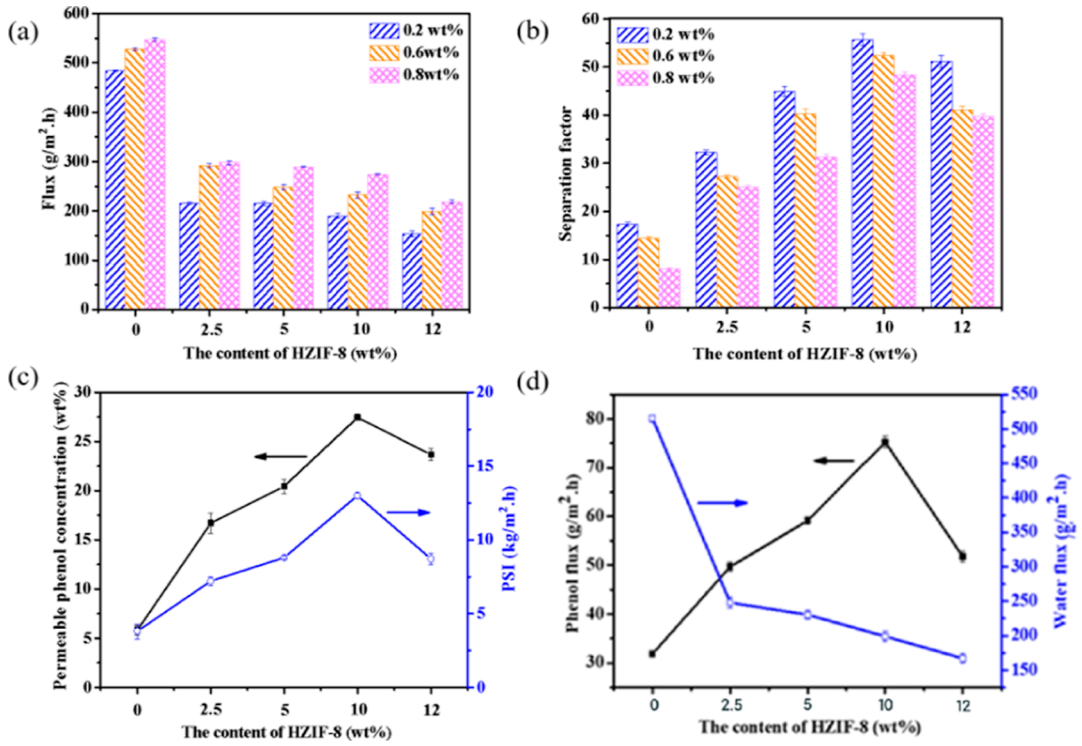

Figure 10. Effect of HZIF-8 content on pervaporation performance of PEBA/HZIF-8 based membranes: (a) total flux and (b) separation factor; effect of HZIF-8 content on (c) PSI and permeate phenol concentration, and (d) phenol and water fluxes with feed phenol concentration of 0.8 wt % and feed temperature 70 °C.

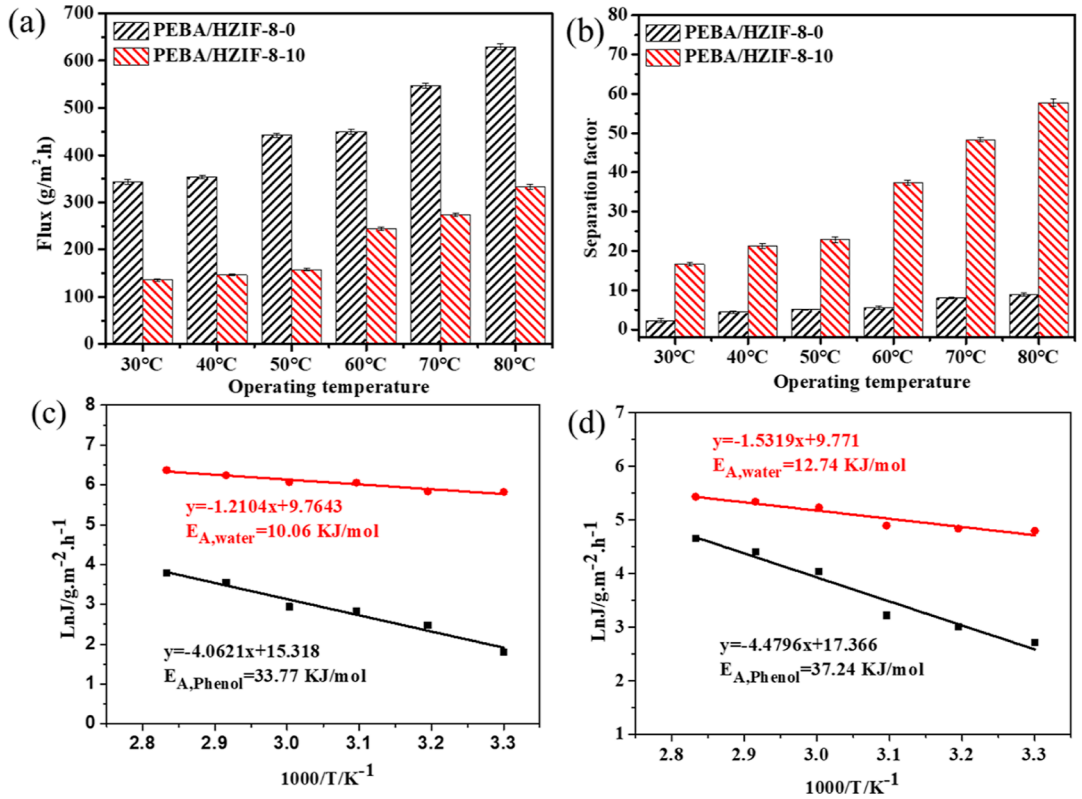

Figure 11. Effect of feed temperature on pervaporation performance of PEBA/HZIF-8-0 and PEBA/HZIF-8-10 membranes: (a) total flux and (b) separation factor; effect of feed temperature on permeate flux of PEBA/HZIF-8-0 (c) and PEBA/HZIF-8-10 (d) membranes.

HZIF-8. This could be attributed to the increased surface roughness and hydrophobicity of PEBA/HZIF-8 based membranes, which led to the increase of the contact area between phenol molecules and HZIF-8 and improved the α_s of the membranes. In addition, the interaction between phenol molecules and PEBA/HZIF-8 based membranes was stronger

https://doi.org/10.1021/acsomega.2c01847
ACS Omega 2022, 7, 23467−23478

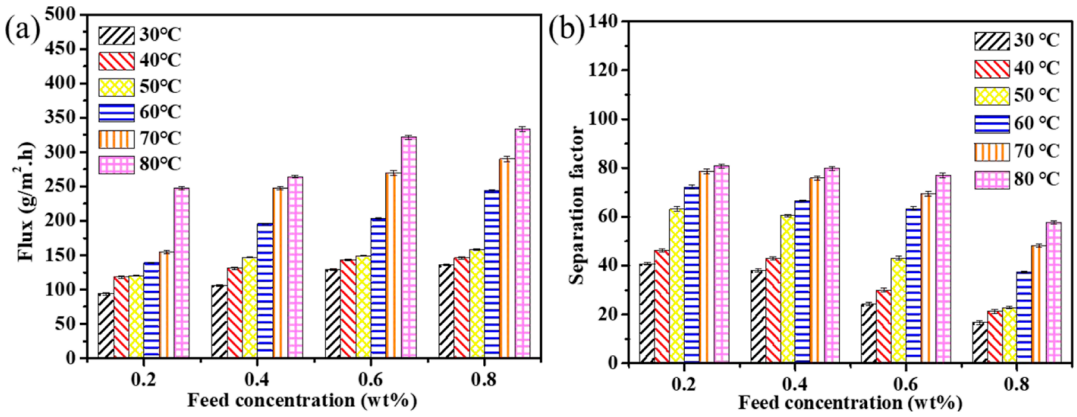

Figure 12. Effect of feed concentration on pervaporation performance of the PEBA/HZIF-8-10 membranes: (a) total flux and (b) separation factor.

than that for water molecules, benefiting the diffusion of phenol molecules in the membranes. However, the α_d of prepared PEBA/HZIF-8 based hybrid membranes was much smaller than that of the α_s, which may be attributed to the smaller size of water molecules compared with that of phenol molecules.

3.2. Pervaporation Test of PEBA/HZIF-8 Based Membranes. *3.2.1. Effect of HZIF-8 Content on Pervaporation Performance of PEBA/HZIF-8 Based Membranes.* Pervaporation performance of PEBA/HZIF-8 based membranes with different HZIF-8 contents under varied feed phenol concentration is shown in Figure 10a,b. Under feed phenol concentration of 0.8 wt % and feed temperature of 70 °C, the separation factor of PEBA/HZIF-8 membranes significantly increased from 8.05 to 48.31 with the increase of HZIF-8 content from 0 to 10 wt % (Figure 10b), while the total flux decreased from 547.53 to 274.12 g/m^2·h (Figure 10a). It was mainly due to the presence of PS on the surface of HZIF-8 and the imidazole ring skeleton in ZIF-8, which enhanced the $\pi-\pi$ interaction between HZIF-8 and phenol molecules and thus promoted the selective adsorption and diffusion of phenol molecules on PEBA/HZIF-8 based membranes. At the same time, the hydrophobic HZIF-8 repels the passage of water molecules, resulting in a decrease in the total flux. When the content of HZIF-8 in the PEBA/HZIF-8 based membranes further increased to 12 wt %, the separation factor of the PEBA/HZIF-8 based membranes decreased. This could be attributed to the formation of non-selective voids in the membrane, which resulted in a decrease in selectivity. In addition, water contact angle values of the PEBA/HZIF-8 membranes had a great impact on the separation factor values of the membrane. This phenomenon further indicates that the increase in hydrophobicity further leads to an increase in the separation factor of the membranes.[48]

As shown in Figure 10c, the PEBA/HZIF-8-10 membrane presented the largest PSI value of 13 kg/m^2·h, and the largest concentration of phenol in the permeable solution of 27.4 wt %, indicating that the PEBA/HZIF-8-10 membrane holds the best pervaporation performance in this series of membranes. It could be seen from Figure 10d that with the increase of HZIF-8 content, the phenol flux of the PEBA/HZIF-8-10 membrane first increased and then decreased, while the water flux kept decreasing. It was concluded that phenol-water clusters were formed by strong hydrogen bonds, which could easily enter the membranes.[10] Therefore, the PEBA/HZIF-8-10 membrane was selected for the subsequent experiment.

3.2.2. Effect of Feed Temperature on Pervaporation Performance of PEBA/HZIF-8 Based Membranes. As shown in Figure 11, both the total flux (Figure 11a) and separation factor (Figure 11b) of PEBA/HZIF-8-0 and PEBA/HZIF-8-10 membranes significantly increased with the increase of feed temperature at the feed phenol concentration of 0.8 wt %. With the increase of feed temperature, the channel between PEBA chains was enlarged and the thermodynamic motion of permeable molecules was accelerated. At the same time, the partial pressure of each component upstream of the membrane was also raised, and therefore, the mass transfer driving force on both sides of the membranes was enhanced, leading to the increase of permeate flux.

The effect of the feed temperature on the flux can be expressed by the Arrhenius equation

$$J_i = J_{o,i}\exp\left(-\frac{E_i}{RT}\right) \quad (7)$$

where J_i (g/m^2·h), $J_{o,i}$ (g/m·h), E_i (J/mol), R (J/mol·k), and T (K) are the permeate flux of component i, the exponential factor, activation energy, molar gas constant, and absolute temperature, respectively. The activation energies of phenol and water ($E_{A,i}$) can be predicted by calculating the slope of linear fitting of the Arrhenius equation. Activation energy is considered to be a sensitive index of permeate flux varying with temperature[29,41] Figure 11c–d showed that the $E_{A,phenol}$ and $E_{A,water}$ of the PEBA/HZIF-8-0 membrane were 33.77 and 10.06 kJ/mol, respectively. The $E_{A,phenol}$ of the PEBA/HZIF-8-10 membrane was 37.24 kJ/mol, and the $E_{A,water}$ was 12.74 kJ/mol. The higher activation energy indicated that change of the permeation flux was greatly affected by temperature. The flux of phenol increased more significantly than the flux of water, and therefore, the selectivity of PEBA/HZIF-8-10 membrane for phenol was improved with rising temperature. As a result, increasing the temperature of the feed was conducive to improving the overall pervaporation performance of the PEBA/HZIF-8 membranes.

3.2.3. Effect of Phenol Concentration on Pervaporation Performance of PEBA/HZIF-8-10 Membranes. As shown in Figure 12a, the total flux of PEBA/HZIF-8-10 membrane increased with the increase of feed phenol concentration under the same feed temperature, while the separation factor decreased accordingly, as displayed in Figure 12b. Due to

https://doi.org/10.1021/acsomega.2c01847
ACS Omega 2022, 7, 23467−23478

Table 1. Comparison of Pervaporation Performance between Different PEBA-Based Membranes for Phenol/Water Separation

membranes	feed concentration (wt %)	feed temperature (°C)	total flux (g/m²·h)	separation factor	PSI (kg/m²·h)	refs
PEBA-2533	0.86	60	610	18	10.37	10
β-CD-f-PEBA-0.5%	0.1	50	319	43	13.40	26
PEBA/PVDF	0.1	80	985	9	7.88	27
PEBA-4033	1	60	620	20	11.78	45
PEBA/MCM-41-4%	0.5	70	1000	35	34.00	46
PEBAX-4033	2	60	350	23	7.70	47
PEBA/HZIF-8-10	0.8	80	333	58	18.98	this paper

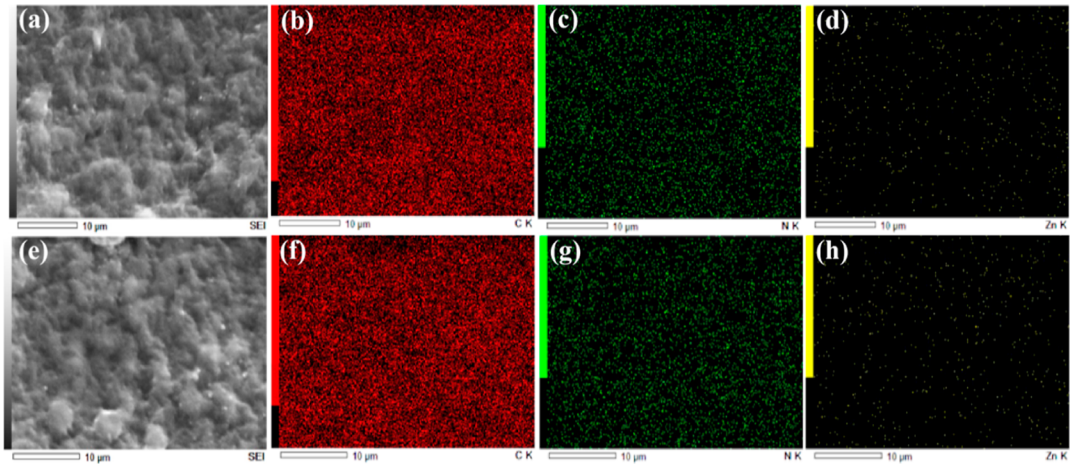

Figure 13. Mapping images of the PEBA/HZIF-8-10 membrane: (a–d) before pervaporation and (e–h) after pervaporation.

strong interactions between the PEBA/HZIF-8-10 membrane and phenol molecules, increase of phenol concentration increased the swelling of the membrane, thus resulting in the enhanced total flux and reduced selectivity of the PEBA/HZIF-8-10 membrane.

To understand the separation performance of our PEBA/HZIF-8-10 membrane, we compared it with various PEBA based membranes reported in the literature, as shown in Table 1. We could find that the selectivity of the PEBA/HZIF-8-10 membrane was better than those of other membranes; however, the flux should be further improved.

3.2.4. Stability Test of PEBA/HZIF-8-10 Membrane. For the industrial application of pervaporation, the long-term stability of the membranes is one of the most important factors.[42,43] The mapping images of PEBA/HZIF-8-10 membrane before and after pervaporation are shown in Figure 13. It could be observed that C, N, and Zn elements on the membrane surface had no significant change before and after pervaporation, indicating that the PEBA/HZIF-8-10 membrane possessed excellent stability.

The stability of the PEBA/HZIF-8-10 membrane was evaluated by the changes of pervaporation performance under the operation in 0.8 wt % phenol aqueous solution at 70 °C for 45 h, as shown in Figure 14. During the experiment, the concentration of phenol in the feed was maintained at a constant state. The selectivity and total flux of PEBA/HZIF-8-10 membrane remained stable, indicating that the PEBA/HZIF-8-10 membrane possessed excellent stability.

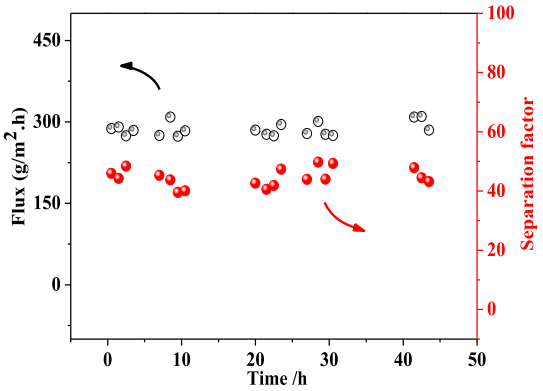

Figure 14. Effect of operation time on pervaporation performance of the PEBA/HZIF-8-10 membrane.

4. CONCLUSIONS

In this study, PEBA/HZIF-8 based membranes were prepared for the recovery of phenol from aqueous solution by pervaporation. The surface morphology, functional groups, and hydrophobicity of PEBA/HZIF-8 membranes were investigated by SEM, AFM, FT-IR, and contact angle methods. The results showed that the water contact angle of PEBA/HZIF-8 based membranes increased obviously with the increase of HZIF-8 content. The hydrophobicity of HZIF-8 was improved by modifying ZIF-8 with PS. The effects of HZIF-8 content, feed phenol concentration, and feed temperature on the separation performance of PEBA/HZIF-8 based membranes were further investigated. The results showed that the modified PEBA membrane with HZIF-8 can significantly improve the pervaporation performance of PEBA/HZIF-8 based membranes. When the feed temperature increased from 30 to 80 °C, the separation factor of the PEBA/HZIF-8-10 membrane increased from 16.65 to 57.73, and the total flux also increased from 136.01 to 333.40 g/m²·h (0.8 wt % feed phenol concentration). When the feed phenol concentration increased from 0.2 to 0.8 wt %, the separation factor of PEBA/

https://doi.org/10.1021/acsomega.2c01847
ACS Omega 2022, 7, 23467−23478

HZIF-8-10 membrane varied from 80.89 to 57.72, and the total flux increased from 247.70 to 333.40 g/m^2·h at 80 °C. In conclusion, the novelty of this work was the synthesis of HZIF-8 by modifying ZIF-8 with PS to improve its hydrophobicity and compatibility with PEBA, and the PEBA/HZIF-8 pervaporation membranes were used for the first time for the separation of phenol/water.

AUTHOR INFORMATION

Corresponding Author

Qian Yang − *College of Chemistry, Chemical Engineering and Environment and Fujian Province University Key Laboratory of Modern Analytical Science and Separation Technology, Minnan Normal University, Zhangzhou 363000, China;* orcid.org/0000-0002-0789-1817; Phone: +86 0596 2591445; Email: yangqian0417@163.com; Fax: +86 0596 2520035

Authors

Yan Xue Xue − *College of Chemistry, Chemical Engineering and Environment, Minnan Normal University, Zhangzhou 363000, China*

Fei Fei Dai − *College of Chemistry, Chemical Engineering and Environment, Minnan Normal University, Zhangzhou 363000, China*

Jian Hua Chen − *College of Chemistry, Chemical Engineering and Environment and Fujian Province University Key Laboratory of Modern Analytical Science and Separation Technology, Minnan Normal University, Zhangzhou 363000, China;* orcid.org/0000-0001-9691-6264

Qiao Jing Lin − *College of Chemistry, Chemical Engineering and Environment, Minnan Normal University, Zhangzhou 363000, China*

Li Jun Fang − *College of Chemistry, Chemical Engineering and Environment, Minnan Normal University, Zhangzhou 363000, China*

Wei Wei Lin − *College of Chemistry, Chemical Engineering and Environment, Minnan Normal University, Zhangzhou 363000, China*

Complete contact information is available at: https://pubs.acs.org/10.1021/acsomega.2c01847

Author Contributions

Y.X.X.: experiment, investigation, methodology, formal analysis, writing the original draft, review, and editing. J.H.C.: investigation, methodology, review, supervision, and editing. F.F.D., Q.J.L., L.J.F., and W.W.L.,: investigation, methodology, review, and editing. Q.Y.: conceptualization, formal analysis, funding acquisition, project administration, resources, supervision, review, and editing.

Notes

The authors declare no competing financial interest.

ACKNOWLEDGMENTS

This work was supported by the National Natural Science Foundation of China (no. 21676133) and Natural Science Foundation of Fujian (nos. 2021J01990 and 2021J05192).

REFERENCES

(1) Cang, W.; Yang, H. Hybrid soft sensor modeling for bisphenol-A synthesis reaction process. *Asia-Pac. J. Chem. Eng.* **2019**, *14*, No. e2378.

(2) Banerjee, P.; Bhattacharya, I.; Chakraborty, T. Cooperative effect on phenolic nuO-H frequencies in 1:1 hydrogen bonded complexes of o-fluorophenols with water: A matrix isolation infrared spectroscopic study. *Spectrochim. Acta Mol. Biomol. Spectrosc.* **2017**, *181*, 116−121.

(3) Chada, R. R.; Enumula, S. S.; Reddy K, S.; Gudimella, M. D.; Rao Kamaraju, S. R.; Burri, D. R. Direct and facile synthesis of $LaPO_4$ containing SBA-15 catalyst for selective O-methylation of phenol to anisole in continuous process. *Microporous Mesoporous Mater.* **2020**, *300*, 110144.

(4) Khabarov, Y. G.; Patrakeev, A. A.; Veshnyakov, V. A.; Kosyakov, D. S.; Ul'yanovskii, N. V.; Garkotin, A. Y. One-step synthesis of picric acid from phenol. *Org. Prep. Proced. Int.* **2017**, *49*, 178−181.

(5) Tang, K.; Zhang, A.; Ge, T.; Liu, X.; Tang, X.; Li, Y. Research progress on modification of phenolic resin. *Mater. Today Commun.* **2021**, *26*, 101879.

(6) Ashraf, H.; Husain, Q. Use of DEAE cellulose adsorbed and crosslinked white radish (Raphanus sativus) peroxidase for the removal of α-naphthol in batch and continuous process. *Int. Biodeterior. Biodegrad.* **2010**, *64*, 27−31.

(7) El-Naas, M. H.; Al-Muhtaseb, S. A.; Makhlouf, S. Biodegradation of phenol by Pseudomonas putida immobilized in polyvinyl alcohol (PVA) gel. *J. Hazard. Mater.* **2009**, *164*, 720−725.

(8) Li, H.; Meng, F.; Duan, W.; Lin, Y.; Zheng, Y. Biodegradation of phenol in saline or hypersaline environments by bacteria: A review. *Ecotoxicol. Environ. Saf.* **2019**, *184*, 109658.

(9) Mirbagheri, N. S.; Sabbaghi, S. A natural kaolin/γ-Fe_2O_3 composite as an efficient nano-adsorbent for removal of phenol from aqueous solutions. *Microporous Mesoporous Mater.* **2018**, *259*, 134−141.

(10) Hao, X.; Pritzker, M.; Feng, X. Use of pervaporation for the separation of phenol from dilute aqueous solutions. *J. Membr. Sci.* **2009**, *335*, 96−102.

(11) Roostaei, N.; Tezel, F. H. Removal of phenol from aqueous solutions by adsorption. *J. Environ. Manage.* **2004**, *70*, 157−164.

(12) Jia, Z.; Wu, G. Metal-organic frameworks based mixed matrix membranes for pervaporation. *Microporous Mesoporous Mater.* **2016**, *235*, 151−159.

(13) El-Naas, M. H.; Al-Zuhair, S.; Alhaija, M. A. Removal of phenol from petroleum refinery wastewater through adsorption on date-pit activated carbon. *Chem. Eng. J.* **2010**, *162*, 997−1005.

(14) Li, Y.; Xing, B.; Wang, X.; Wang, K.; Zhu, L.; Wang, S. Nitrogen-doped hierarchical porous biochar derived from corn stalks for phenol enhanced adsorption. *ACS Omega* **2019**, *33*, 12459−12468.

(15) Wu, D.; Chen, G. Q.; Hu, B.; Deng, H. Feasibility and energy consumption analysis of phenol removal from salty wastewater by electro-electrodialysis. *Separ. Purif. Technol.* **2019**, *215*, 44−50.

(16) Vaiano, V.; Matarangolo, M.; Murcia, J. J.; Rojas, H.; Navío, J. A.; Hidalgo, M. C. Enhanced photocatalytic removal of phenol from aqueous solutions using ZnO modified with Ag. *Appl. Catal., B* **2018**, *225*, 197−206.

(17) Malina, N.; Wei, X.; Kümmel, S.; Richnow, H. H.; Vogt, C. Analysis of carbon and hydrogen stable isotope ratios of phenolic compounds: method development and biodegradation applications. *ACS Omega* **2021**, *2*, 32−39.

(18) Wang, Y.; Chen, H.; Liu, Y.-X.; Ren, R.-P.; Lv, Y.-K. An adsorption-release- biodegradation system for simultaneous biodegradation of phenol and ammonium in phenol-rich wastewater. *Bioresour. Technol.* **2016**, *211*, 711−719.

(19) Zhang, H.; James, J.; Zhao, M.; Yao, Y.; Zhang, Y.; Zhang, B.; Lin, Y. S. Improving hydrostability of ZIF-8 membranes via surface ligand exchange. *J. Membr. Sci.* **2017**, *532*, 1−8.

(20) Barlak, M. S.; Değermenci, N.; Cengiz, İ.; Ucun Özel, H.; Yildiz, E. Comparison of phenol removal with ozonation in jet loop reactor and bubble column. *J. Environ. Chem. Eng.* **2020**, *8*, 104402.

(21) Liu, Y.; Zhang, J.; Tan, X. High performance of PIM-1/ZIF-8 composite membranes for O_2/N_2 separation. *ACS Omega* **2019**, *4*, 16572−16577.

(22) Li, D.; Liu, B.; Sun, H.; Yao, J.; van Agtmaal, S.; Feng, C. Preparation and characterization of PFTS grafted alumina supported zirconia (ASZ) membrane for removal of phenol from aqueous solution. *Appl. Surf. Sci.* **2020**, *505*, 144608.
(23) He, Q.-P.; Zou, Y.; Wang, P.-F.; Dou, X.-m. MFI-type zeolite membranes for pervaporation separation of dichlorobenzene isomers. *ACS Omega* **2021**, *6*, 8456−8462.
(24) Ong, Y. K.; Shi, G. M.; Le, N. L.; Tang, Y. P.; Zuo, J.; Nunes, S. P.; Chung, T.-S. Recent membrane development for pervaporation processes. *Prog. Polym. Sci.* **2016**, *57*, 1−31.
(25) Cao, X.; Wang, K.; Feng, X. Removal of phenolic contaminants from water by pervaporation. *J. Membr. Sci.* **2021**, *623*, 119043.
(26) Zhang, S.; Zou, Y.; Wei, T.; Mou, C.; Liu, X.; Tong, Z. Preparation of β-cyclodextrin/polyether copolyacetamide filled membrane and separation of trace phenol in water by permeation vaporization. *J. Chem. Eng.* **2016**, *67*, 9−18.
(27) Khan, R.; Haq, I.; Mao, H.; Zhang, A.; Xu, L.; Zhen, H.; Zhao, Z. Enhancing the pervaporation performance of PEBA/PVDF membrane by incorporating MAF-6 for the separation of phenol from its aqueous solution. *Sep. Purif. Technol.* **2020**, *256*, 117804.
(28) Sutrisna, P. D.; Hou, J.; Zulkifli, M. Y.; Li, H.; Zhang, Y.; Liang, W.; D'Alessandro, D. M.; Chen, V. Surface functionalized UiO-66/Pebax-based ultrathin composite hollow fiber gas separation membranes. *J. Mater. Chem. A* **2018**, *6*, 918−931.
(29) Zheng, H.; Wang, D.; Sun, X.; Jiang, S.; Liu, Y.; Zhang, D.; Zhang, L. Surface modified by green synthetic of Cu-MOF-74 to improve the anti-biofouling properties of PVDF membranes. *Chem. Eng. J.* **2021**, *411*, 128524.
(30) Adoor, S. G.; Manjeshwar, L. S.; Bhat, S. D.; Aminabhavi, T. M. Aluminum-rich zeolite beta incorporated sodium alginate mixed matrix membranes for pervaporation dehydration and esterification of ethanol and acetic acid. *J. Membr. Sci.* **2018**, *318*, 233−246.
(31) Furukawa, S.; Reboul, J.; Diring, S.; Sumida, K.; Kitagawa, S. Structuring of metal-organic frameworks at the mesoscopic/macroscopic scale. *Chem. Soc. Rev.* **2014**, *43*, 5700−5734.
(32) Li, B.; Chrzanowski, M.; Zhang, Y.; Ma, S. Applications of metal-organic frameworks featuring multi-functional sites. *Coord. Chem. Rev.* **2016**, *307*, 106−129.
(33) Sasikumar, B.; Bisht, S.; Arthanareeswaran, G.; Ismail, A. F.; Othman, M. H. D. Performance of polysulfone hollow fiber membranes encompassing ZIF-8, SiO_2/ZIF-8, and amine-modified SiO_2/ZIF-8 nanofillers for CO_2/CH_4 and CO_2/N_2 gas separation. *Separ. Purif. Technol.* **2021**, *264*, 118471.
(34) Amedi, H. R.; Aghajani, M. Aminosilane-functionalized ZIF-8/PEBA mixed matrix membrane for gas separation application. *Microporous Mesoporous Mater.* **2017**, *247*, 124−135.
(35) Amedi, H. R.; Aghajani, M. Modified zeolitic-midazolate framework 8/poly (ether-block-amide) mixed-matrix membrane for propylene and propane separation. *J. Appl. Polym. Sci.* **2018**, *135*, 46273−46286.
(36) Sarwar, Z.; Tichonovas, M.; Krugly, E.; Masione, G.; Abromaitis, V.; Martuzevicius, D. Graphene oxide loaded fibrous matrixes of polyether block amide (PEBA) elastomer as an adsorbent for removal of cationic dye from wastewater. *J. Environ. Manage.* **2021**, *298*, 113466.
(37) Chen, J. H.; Su, Z. B.; Xu, J. P.; Lin, L. J.; Dong, X. F.; Peng, Q.; He, Y. S.; Nie, Y. J. Fabrication of PEBA/Cu_2O mixed-matrix membranes and their application in pyridine recovery from aqueous solution. *RSC Adv.* **2017**, *7*, 22936−22945.
(38) Bustamante, E. L.; Fernández, J. L.; Zamaro, J. M. Influence of the solvent in the synthesis of zeolitic imidazolate framework-8 (ZIF-8) nanocrystals at room temperature. *J. Colloid Interface Sci.* **2014**, *424*, 37−43.
(39) Zhu, T.; Xu, S.; Yu, F.; Yu, X.; Wang, Y. ZIF-8@GO composites incorporated polydimethylsiloxane membrane with prominent separation performance for ethanol recovery. *J. Membr. Sci.* **2020**, *598*, 117681.
(40) Cravillon, J.; Münzer, S.; Lohmeier, S.-J.; Feldhoff, A.; Huber, K.; Wiebcke, M. Rapid room-temperature synthesis and characterization of nanocrystals of a prototypical zeolitic imidazolate framework. *Chem. Mater.* **2009**, *21*, 1410.
(41) Khulbe, K. C.; Matsuura, T. Characterization of synthetic membranes by Raman spectroscopy, electron spin resonance, and atomic force microscopy; a review. *Polymer* **2000**, *41*, 1917−1935.
(42) Zhang, M.; Zhang, Z.; Liu, S.; Peng, Y.; Chen, J.; Ki, S. Y. Ultrasound-assisted electrochemical treatment for phenolic wastewater. *Ultrason. Sonochem.* **2020**, *65*, 105058.
(43) Amirkhani, F.; Mosadegh, M.; Asghari, M.; Parnian, M. J. The beneficial impacts of functional groups of CNT on structure and gas separation properties of PEBA mixed matrix membranes. *Polym. Test.* **2020**, *82*, 106285.
(44) Peng, J.; Zhang, S. Y.; Chen, W.; Wang, L.; Wei, S.; Peng, C. A macroporous metal-organic framework with enhanced hydrophobicity for efficient oil adsorption. *Chem.—Eur. J.* **2018**, *24*, 3754−3759.
(45) Böddeker, K. W.; Bengtson, G.; Bode, E. Pervaporation of low volatility aromatics from water. *J. Membr. Sci.* **1990**, *53*, 143−158.
(46) Wang, M.; Zhang, X.; Li, X.; Hao, X.; Li, C.; Ding, C.; Wang, Q. Preparation of PEBA/MCM-41 hybrid membrane and its pervaporation separation performance of phenol/water. *Membr. Sci. Technol.* **2015**, *35*, 40−47.
(47) Kujawski, W.; Warszawski, A.; Ratajczak, W.; Porębski, T.; Capała, W.; Ostrowska, I. Application of pervaporation and adsorption to the phenol removal from wastewater. *Sep. Purif. Technol.* **2004**, *40*, 123−132.
(48) Choudhari, S. K.; Cerrone, F.; Woods, T.; Joyce, K.; Flaherty, V. O.; Connor, K. O.; Babu, R. Pervaporation separation of butyric acid from aqueous and anaerobic digestion (AD) solutions using PEBA based composite membranes. *J. Ind. Eng. Chem.* **2015**, *23*, 163−170.

https://doi.org/10.1021/acsomega.2c01847
ACS Omega 2022, 7, 23467−23478